

Theoretical and Experimental Study on Ion-Pair Formation and Partitioning of Organic Salts in Octanol/Water and Dichloromethane/Water Systems

Peter I. Nagy^{a*} and Krisztina Takács-Novák^{b*}

Contribution from the Department of Medicinal and Biological Chemistry, The University of Toledo, Toledo, Ohio 43606-3390, and Institute of Pharmaceutical Chemistry, Semmelweis University, H-1092 Budapest, Hungary

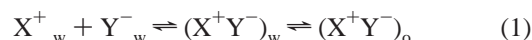
Received January 31, 2000

Abstract: A good linear correlation ($r = 0.945$) of the octanol/water and dichloromethane/water $\log P'$ values has been found for quaternary amines with organic counterions. Monte-Carlo simulation based potential of mean force curves (PMF) for medium and large quaternary amine cations, and small and medium size anions show partially different characters in dichloromethane (DCM) solvent. The PMFs show, with one exception, both locally stable contact and solvent-separated ion-pair arrangements. The solvent-separated form is at least as stable as the contact ion-pair. Consideration of two water molecules at the interaction sites of the ionic heads remarkably lowers the activation free energy toward the formation of the contact ion arrangement. The quaternary substitution of the nitrogen prevents hydrogen bonding to the cation at its most positive site. Secondary acceptor sites can still be important, but at larger separations the water molecules always formed strong hydrogen bonds only at the $-\text{COO}^-$ and $-\text{SO}_3^-$ anionic sites. Stability of the contact ion-pair is enhanced by a water-bridged hydrogen-bond network possible only at small ion separations in DCM. According to a suggested putative model for ion-pair partitioning between water and DCM, the anion enters the organic phase and drags some water molecules. The cation separated by about 8–10 Å follows the hydrated anion in the organic phase. A mixture of the contact and solvent separated ion-pairs in DCM is preferably formed if the free energy difference does not exceed 2 kcal/mol, and the activation free energy of the contact ion-pair formation is no more than about 3 kcal/mol, as calculated for some ion-pairs here.

Introduction

While structure and thermodynamics of aqueous ionic solutions have been studied both experimentally and theoretically (including computer modeling) for a long time,¹ much less interest has been paid for ions and ion-pairs in organic solvents. Nonetheless, since the early 20's, when Bjerrum developed the theory of the ion-pair formation between oppositely charged ions in low dielectric-constant solvents,² formation and partition of ion-pairs have been broadly applied in analytical procedures as ion-pair extraction titrimetric methods,³ ion-exchange techniques,⁴ and later in ion-pair chromatography.⁵

Schanker et al.⁶ proposed for the first time in medicinal chemistry an ion-pair partition based drug absorption theory as a possible alternative for the transport of permanent ions (e.g. quaternary ammonium salts, QA), or drugs which are largely ionized at any pH in the living organism (e.g. strong bases, peptides). This concept was introduced to resolve the obvious contradiction within the pH-partition theory⁷ generally accepted for the absorption/distribution mechanism of drugs. By simply assuming a passive transport, the penetration of neutral molecules and nonionized weak electrolytes in lipophilic phases can be successfully explained. The theory fails, however, to elucidate the absorption behavior of ionized drugs. According to the ion-pair absorption mechanism, the hydrophilic pharmacion (cation or anion) and an appropriate counterion form a less polar, more lipophilic species, and the dimer partitions through the lipid bilayer of membranes⁸ as a stable ion-pair, (X^+Y^-) . (Indices w and o in eqs 1 and 2 stand for the aqueous and slightly polar organic phases, respectively, P' and P correspond to the apparent and true partition coefficients, respectively.)



$$P' = [(\text{X}^+\text{Y}^-)]_o / ([\text{X}^+]_w + [(\text{X}^+\text{Y}^-)]_w) \quad (2a)$$

$$P = [(\text{X}^+\text{Y}^-)]_o / [(\text{X}^+\text{Y}^-)]_w \quad (2b)$$

Due to the lack of exact in vivo experimental evidences, the ion-pair absorption mechanism of drugs was refused by many

[†] The University of Toledo.

[‡] Semmelweis University.

(1) See, e.g.: (a) Ben Naim, A. *Ionic Solutions*; Plenum: New York, 1980. (b) Marcus, Y. *Ion Solvation*; Wiley: New York, 1985. (c) Bopp, P. In *The Physics and Chemistry of Aqueous Ionic Solutions*; Bellissent, M.-C., Neilson, G. W., Eds.; Reidel: Dordrecht, 1987; p 217. (d) Hubbard, J.; Wolynes, P. In *The Chemical Physics of Ion Solvation, Part C*; Dogonadze, R. R., Kalman, E., Kornyshev, A. A., Ulstrup, J., Eds.; Elsevier: New York, 1988. (e) Heinzinger, K. In *Molecular Dynamics Simulations of Aqueous Systems in Computer Modeling of Fluids, Polymers and Solids*; Catlow, C. R. A., Parker, S. C., Allen, M. P., Eds.; Kluwer: Dordrecht, 1990; p 357. (f) March, J. In *Advanced Organic Chemistry*, 4th ed.; John Wiley & Sons: New York, 1992; p 293.

(2) Bjerrum, N. *Kgl. Danske Selskab.* **1926**, 7, 9.

(3) Bult, A. In *Topics in Pharmaceutical Sciences 1983*; Breimerand, D. D., Speiser, P., Eds.; Elsevier: Amsterdam, 1983.

(4) Inczédy, J. *Analytical Application of Ion Exchangers*; Academic Press: Budapest, 1966.

(5) Hearn, M. T. W. *Ion-pair Chromatography*; Marcel Dekker: New York, 1985.

authors.^{9,10} Recently, however, the ion-pair formation has attracted attention again as a possible improvement of the low lipophilicity, and thus inadequate absorption of peptides and peptidomimetics type potential pharmacons.⁸

As far as the solvent effects are concerned, ion-pairs can only be formed in solution if a critical distance of separation,¹¹ inverse proportional to the dielectric constant of the solvent (Bjerrum rule), has been reached. The resulting ion-pairs exhibit stable, thermodynamically distinct species, and can exist either in contact (tight, intimate) or solvent-separated (loose) ion-pair, depending on the strength of the solvent–ion interactions.^{12–14} If the interacting free ions have a sufficiently tight solvation shell, and their associate maintains this structure, a solvent-separated, loose ion-pair will be formed. In other cases contact ion-pairs are produced. It is important to emphasize that Bjerrum's original definition referred to solvent-separated ion-pairs held together by electrostatic attraction (Bjerrum or electrostatic type ion-pairs). In 1963 Diamond¹⁵ defined the "water-structure enforced ion-pair", which is formed by participation of two large hydrophobic ions. In these systems hydrophobic forces and H-bonding also support the pair formation. This kind of ion-pairs, also called "hydrophobic ion-pairing" (HIP), may exist both in water and in other highly structured polar solvents. The HIP complexes, by taking mainly the contact form, display enhanced lipophilicity, and thus are better suited for their potentially important, pharmacology related application as mentioned above.

Much less is known about the chemical and geometric aspects of the interacting ions favoring the pair formation. Large organic species are more ready for ion-pairing than small inorganic ones,¹⁶ the size of the interacting ions seems to have a determining role.¹⁷ So far only a small amount of information has been accumulated on how the functional groups in an organic molecule contribute to the ion-pair formation. Recently, Takács-Novák and Szász reported an extensive shake-flask partition study¹⁸ and also HPLC investigations¹⁹ on the ion-pair partition of quaternary ammonium cations, examining the role of 10 counterions of different size, shape, flexibility, and lipophilicity. Both the octanol/water and the reversed phase chromatographic partition mechanisms were interpreted as involving hydrophobic interactions and H-bond formation, and the influence of the ion flexibility has been invoked for explaining the experimental results.

The goal of the present study is a computer-modeling investigation of the structural conditions of ion-pair formation in a moderately polar solvent and aqueous solution. Effects of the ion-size and hydrogen-bonding capacity on the formation of contact ion-pairs have been studied and analyzed in com-

parison with experimental log P' values measured in octanol/water and dichloromethane/water systems. Quaternary amines were intentionally selected as cations, because this chemical structure ensures the conservation of the positive charge in any solvents and associates. Amines up to tertiary substitution are generally protonated in aqueous solutions, but it is not clear how much of this state is maintained after entering the organic phase.

Experimental Section

Materials. Propantheline bromide (PROP) was obtained from Chinoin Pharm. Ltd. (Budapest, Hungary) and deramcyclane was supplied by EGIS Pharmaceuticals (Budapest, Hungary). Homidium bromide (ethidium bromide, HOM) and neostigmine bromide (NEOST) were purchased from Sigma-Aldrich Chemie (Germany). *N*-Methyl-deramcyclane (MeDER) was prepared from deramcyclane and *N*-methylquinidine (MeCHIN) was synthesized from quinidine in our lab using the standard quaternization reaction with CH_3I . The QA compounds were used without further purification. Materials used as counterions were also purchased from Sigma-Aldrich either in acid (fumaric, *p*-toluenesulfonic, and nicotinic acids) or in salt form (sodium acetate, caproate, pyruvate, and deoxycholate). Prostaglandin E_1 was generously gifted by Chinoin. All other reagents were of analytical grade. The *n*-octanol and dichloromethane were of HPLC grade (Sigma-Aldrich).

Partition Coefficient Determination. The shake-flask method was applied for log P measurements of ion-pairs in both octanol/water (*o/w*) and dichloromethane/water (DCM/*w*) solvent systems, where Sørensen buffer, pH 7.4, served as the aqueous phase. The octanol/water measurements have been carried out at increasing molar ratio of the counterion in the range of 1:1 and 50:1, as described previously.¹⁸ In this paper the apparent partition coefficients (log $P'_{o/w}$) obtained at a 50:1 molar ratio of the counterion and QA are used for the correlation study. Measurements in the DCM/*w* system were carried out using identical circumstances (25 °C, $I = 0.27 \text{ M}$, 50:1 molar ratio). The mutual saturation of the two phases was achieved by stirring them intensively for 6 h at 25 °C and allowing them to stand overnight. Each quoted log P' value is an average of a minimum of four and generally six parallel measurements. The standard deviations (SD) of the results were less than 0.05 log units.

Water Content Determination. The standard Karl Fischer method was used for determination of the water content in saturated dichloromethane at 25 °C.

Computational Methods

The potential of mean force (PMF) has been calculated for several ion-pairs (Chart 1: trimethylaniline–acetate (TMA/AC), trimethylaniline–hydrogenfumarate (TMA/HFUM), homidium–hydrogenfumarate (HOM/HFUM), homidium–*p*-toluenesulfonate (HOM/PTS), *N*-methyl-deramcyclane–hydrogenfumarate (MeDER/HFUM)) and for the water dimer in dichloromethane solvent. PMF for the HOM/PTS system was also studied in aqueous solution.

PMFs were calculated using the free energy perturbation method as applied in Monte-Carlo simulations.²⁰ Calculations were performed by using the BOSS Version 3.6 program²¹ implemented to a Silicon Graphics Indigo2 workstation at the University of Toledo. NpT isobaric–isothermal ensembles were considered at $p = 1 \text{ atm}$ and $T = 298$. Systems consisted of the ion-pair, 250–255 dichloromethane molecules, and two water molecules. The three-point DCM model of Lim et al.²² was taken from this program. The TIP4P water model²³ was used both in calculations with the DCM solvent and in the aqueous solution simulations for the HOM/PTS ion-pair surrounded by 479 water molecules.

(20) Jorgensen, W. L.; Ravimohan, C. *J. Chem. Phys.* **1985**, *83*, 3050.

(21) Jorgensen, W. L. BOSS, Version 3.6, *Biochemical and Organic Simulation System User's Manual*; Yale University: New Haven, CT, 1995.

(22) Lim, D.; Hrovat, D. A.; Borden, W. T.; Jorgensen, W. L. *J. Am. Chem. Soc.* **1994**, *116*, 3494.

(23) (a) Jorgensen, W. L.; Chandrasekhar, J.; Madura, J. D.; Impey, R. W.; Klein, M. L. *J. Chem. Phys.* **1983**, *79*, 926. (b) Jorgensen, W. L.; Madura, J. D. *Mol. Phys.* **1985**, *56*, 1381.

(6) Schanker, L. S. *J. Med. Pharm. Chem.* **1960**, *2*, 343.

(7) Shore, P. A.; Brodie, B. B.; Hogben, G. A. M. *J. Pharmacol. Exp. Ther.* **1957**, *119*, 361.

(8) Neubert, R. *Pharm. Res.* **1989**, *6*, 743.

(9) Jonkman, J. H. G.; Hunt, C. A. *Pharm. Weekbl. [Sci.]* **1982**, *5*, 41.

(10) Austin, R. P.; Davis, A. M.; Manners, C. N. *J. Pharm. Sci.* **1995**, *84*, 1180.

(11) Kraus, C. A. *J. Phys. Chem.* **1956**, *60*, 129.

(12) Sadek, H.; Fuoss, R. M. *J. Am. Chem. Soc.* **1954**, *76*, 5897.

(13) Winstein, S.; Clippinger, E.; Fainberg, A. H.; Robinson, G. C. *J. Am. Chem. Soc.* **1954**, *76*, 2597.

(14) Roberts, R. C.; Szwarc, M. *J. Am. Chem. Soc.* **1965**, *87*, 5542.

(15) Diamond, R. M. *J. Phys. Chem.* **1963**, *67*, 2513.

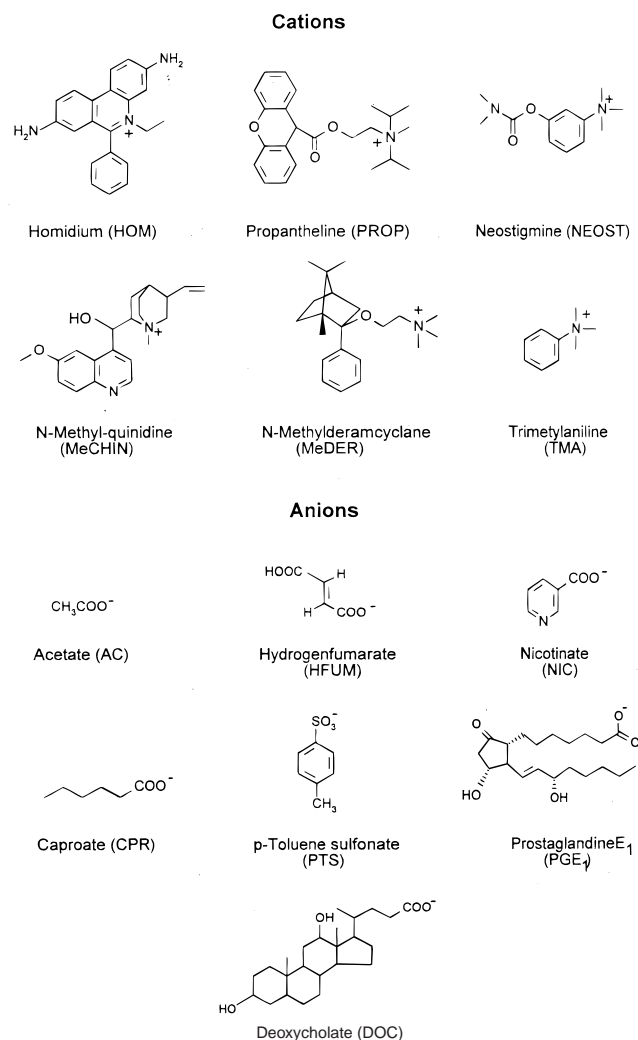
(16) Fini, A.; Fazio, G.; Gonzalez-Rodriguez, M.; Cavallari, C.; Passerini, N.; Rodriguez, L. *Int. J. Pharm.* **1999**, *187*, 163.

(17) Quintanar-Guerrero, D.; Allemann, E.; Fessi, H.; Doelker, E. *Pharm. Res.* **1997**, *14*, 119.

(18) Takács-Novák, K.; Szász, Gy. *Pharm. Res.* **1999**, *16*, 1633.

(19) Szász, Gy.; Takács-Novák, K. *J. Chromatogr. B*. Accepted for publication.

Chart 1



Starting from an equilibrated ca. $30 \times 30 \times 30 \text{ \AA}^3$ DCM box, 12–17 solvent molecules were deleted because of poor contacts with the solutes. Ion geometries were optimized at the HF/6-31G* level for cations and at the HF/6-31+G* level for anions,²⁴ using the Gaussian 94 software²⁵ running on a T90 machine at the Ohio Supercomputer Center. Reasonable starting geometries led to local energy minima (confirmed by normal frequency analysis) for all ions. For the MeDER cation the trans O–C–C–N conformer was accepted. The PMFs were taken by changing the *R* distance between the cationic center, N, and the carboxylic C atom of the anion or C_{ring} (connecting to S) in PTS. Two water molecules were placed between the ion-pairs, allowing formation of hydrogen bonds to anionic oxygens.

Periodic boundary conditions with the nearest image approximation and preferential sampling were applied. The probability of a new configuration upon solvent move is proportional to $1/(R^2 + c)$, where *R* is the distance between the central atom of the solvent and the ion-pair center. This latter was defined at halfway between the cationic N atom and the C atom in the anion. The *c* constant was set to 250 and 120 in DCM and water, respectively. Solute moves were tried every

(24) Hehre, W. J.; Radom, L.; Schleyer, P. v. R.; Pople, J. A. *Ab Initio Molecular Orbital Theory*; Wiley: New York, 1986.

(25) Gaussian 94, Revision E. 2. Frisch, M. J.; Trucks, G. W.; Schlegel, H. B.; Gill, P. M. W.; Johnson, B. G.; Robb, M. A.; Cheeseman, J. R.; Keith, T.; Petersson, G. A.; Montgomery, J. A.; Raghavachari, K.; Al-Laham, M. A.; Zakrzewski, V. G.; Ortiz, J. V.; Foresman, J. B.; Cioslowski, J.; Stefanov, B. B.; Nanayakkara, A.; Challacombe, M.; Peng, C. Y.; Ayala, P. Y.; Chen, W.; Wong, M. W.; Andres, J. L.; Replogle, E. S.; Gomperts, R.; Martin, R. L.; Fox, D. J.; Binkley, J. S.; Defrees, D. J.; Baker, J.; Stewart, J. P.; Head-Gordon, M.; Gonzalez, C.; Pople, J. A. Gaussian, Inc.: Pittsburgh, PA, 1995.

50 steps. The elements of the ion-pair were rigidly translated in these moves but separate rotations were allowed for the cation or the anion about a random axis through the reference N or C atoms, respectively. The two water molecules were moved independently of each other and the ion-pair. Volume changes were tried every 1000 steps. Equilibration and averaging was taken by considering 3500K and 5000K configurations, respectively. The perturbation step was 0.05–0.2 Å in PMF calculations, using double-wide sampling. The solvent–solvent cutoff radius was set to 14 and 8.5 Å in DCM and aqueous solution, respectively. The ICUT = 2 option was used for the solute–solvent cutoff, allowing consideration of interactions with any solvent molecules within 15 Å and 12 Å spheres of any explicit solute atoms in DCM and water, respectively. Solute atoms were explicitly considered except the elements of the CH_{*n*} (*n* = 1, 2, 3) groups where the united atom model was applied. The solute–solute interaction was fully considered at any separations, applying the nearest image approximation. Long-range electrostatic effects were considered as nearly constant throughout the calculations. At the applied large solute–solvent cutoff radii the generalized Born formula is a reasonable approximation,²⁶ which provides, however, a constant energy term at any separation of the ion-pair with rigid geometry and fixed atomic charges.

Intermolecular interactions were calculated by using the 12-6-1 OPLS potential.²⁷ Steric parameters were taken from the program's library. Net atomic charges, calculated by use of the CHELPG procedure,²⁸ were obtained upon fitting a set of atom-centered charges to the molecular electrostatic potential. For the anions both the HF/6-31G* and HF/6-31+G* potential derived net charges were determined. On the basis of the HF/6-31+G* wave function, the fitted atomic charges led to more polarized COO[−] and SO₃[−] groups than those obtained by using the HF/6-31G* wave function. A PMF study for the TMA/AC system showed minor difference with the two sets. Thus, in other calculations the theoretically more sound, HF/6-31+G* electrostatic potential fitted charges were used.

Results and Discussion

Ion-Pair Partition in Octanol/Water and DCM/Water. The logarithm of the *n*-octanol/water partition coefficient is widely used in QSAR studies,²⁹ even though there is no solid theoretical basis why this specific solvent and related log *P* should have this particular interest. The linear correlation of the log *P* values obtained for neutral solutes with different organic solvents was recognized a long time ago.³⁰ Due to the lack of a solvent box, theoretical modeling of octanol solutions is not possible by Monte-Carlo simulations using BOSS 3.6. The dichloromethane solvent with the dielectric constant close to that of *n*-octanol ($\epsilon = 8.93$ and 10.30, respectively³¹) may be taken as a moderately polar solvent, but the water-saturated solution structures are very different.

Second-harmonic generation of laser light experiments³² and molecular dynamic simulation³³ of the water/octanol interface found the octanol OH pointing toward the aqueous phase. X-ray diffraction experiments³⁴ and molecular dynamics simulations

(26) See, e.g.: (a) Constanciel, R.; Contreras, R. *Theor. Chim. Acta* **1984**, 65, 1. (b) Kozaki, T.; Morihashi, K.; Kikuchi, O. *J. Am. Chem. Soc.* **1989**, 111, 1547. (c) Still, W. C.; Tempczyk, A.; Hawley, R. C.; Hendrickson, T. *J. Am. Chem. Soc.* **1990**, 112, 6127. (d) Cremer, C. J.; Truhlar, D. G. *Science* **1992**, 256, 213. (e) Hawkins, G. D.; Cremer, C. J.; Truhlar, D. G. *J. Phys. Chem.* **1996**, 100, 19824.

(27) Tirado-Rives, J.; Jorgensen, W. L. *J. Am. Chem. Soc.* **1988**, 110, 1657.

(28) Breneman, C. M.; Wiberg, K. B. *J. Comput. Chem.* **1990**, 11, 316.

(29) (a) Silverman, R. B. *The Organic Chemistry of Drug Design and Drug Action*; Academic Press: San Diego, 1992. (b) *3D QSAR in Drug Design*; Kubinyi, H., Ed.; ESCOM: Leiden, 1993.

(30) Leo, A.; Hansch, C.; Elkins, D. *Chem. Rev.* **1971**, 71, 525.

(31) *CRC Handbook of Chemistry and Physics*, 80th ed.; CRC Press LLC: Boca Raton, FL, 1999.

(32) Cramb, D. T.; Wallace, S. C. *J. Phys. Chem. B* **1997**, 101, 2741.

(33) Michael, D.; Benjamin, I. *J. Phys. Chem.* **1995**, 99, 16810.

(34) Franks, N. P.; Abraham, M. H.; Lieb, W. R. *J. Pharm. Sci.* **1993**, 82, 466.

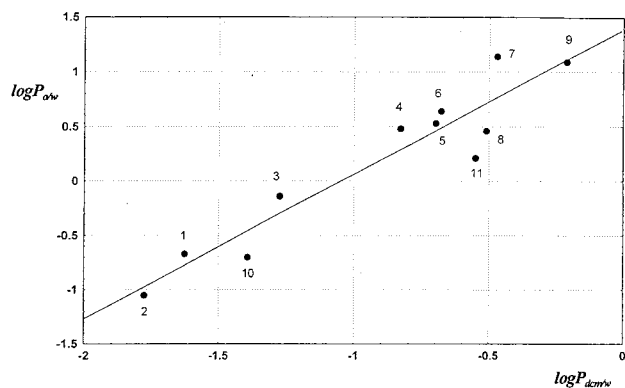


Figure 1. Correlation of the $\log P'$ (octanol/water) and $\log P'$ (dichloromethane/water) values.

Table 1. Lipophilicity Data of Ion-Pairs in Octanol/Water and Dichloromethane/Water Systems at a 1:50 Molar Ratio of QA/Y

ion-pairs	$\log P'$		ion-pairs	$\log P'$	
	o/w	DCM/w		o/w	DCM/w
HOM-AC	-0.67	-1.63	PROP-CPR	0.64	-0.68
HOM-HFUM	-1.05	-1.78	PROP-DOC	1.14	-0.47
HOM-NIC	-0.14	-1.27	MeCHIN-CPR	0.46	-0.51
HOM-CPR	0.48	-0.83	MeCHIN-PGE ₁	1.09	-0.21
HOM-PTS	0.53	-0.70	NEOST-DOC	-0.70	-1.39
			MeDER-CPR	0.21	-0.55

for the pure and water-saturated octanol^{35,36} indicate that the octanol molecules assume a fairly extended structure in general. The CCC arrangement is trans in about 75% of conformers of the pure liquid octanol.³⁵ In the water-saturated octanol a maximum of about 16 octanol molecules form an aggregate, and water molecules are surrounded by the OH groups of these clusters.³⁴

The dichloromethane–water liquid–liquid interface has been recently studied by Dang.³⁷ The MD calculations predicted good bulk densities, and pointed out that the water and DCM densities decrease from their bulk values to nearly zero in a layer with a thickness of about 8 Å. This means that very low water concentration is expected beyond the interface. Indeed, our measured water content is 0.135 g in 100 mL of DCM, which corresponds to a molar ratio of about 1:208 at $T = 298$ °C. These results altogether suggest that water molecules do not penetrate deeply in DCM if the two systems are in equilibrium.

Despite the above structural differences, significant linear correlation has been found (Figure 1) for the $\log P'_{o/w}$ and $\log P'_{DCM/w}$ values considering 11 different combinations of five cations and seven anions listed in Table 1:

$$\log P'_{o/w} = 1.329(\pm 0.153) \log P'_{DCM/w} + 1.392(\pm 0.158) \quad (3)$$

$$n = 11, r = 0.945, s = 0.16, F = 75.3$$

The correlation suggests that conclusions derived from theoretical modeling of medium size ion-pairs in DCM may be cautiously extended, and can provide starting points for characterization of ion-pairs in other solvents (e.g. octanol).

The focus of Dang's above study is on the DCM/water interface. What happens, however, if the aqueous and DCM phases are separated after the partition equilibrium has been

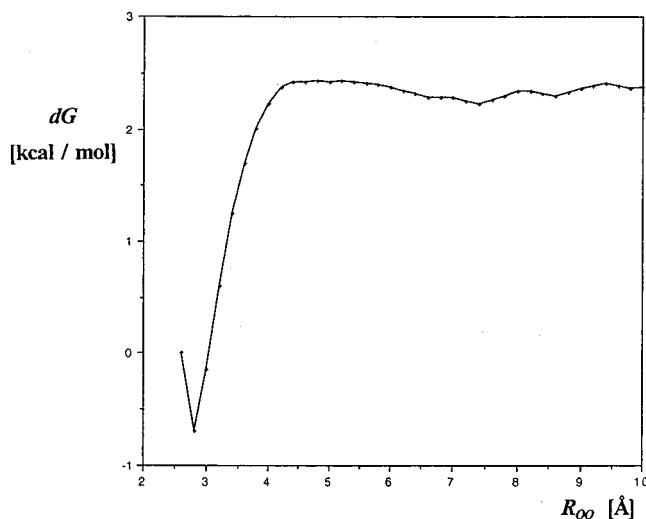


Figure 2. PMF for the water dimer in DCM.

achieved, as happens when using the shake-flask method for determining the concentration of the partitioned organic salt?

It has been demonstrated in our studies that the considered ion-pairs enter the organic phase. Osakai et al.³⁸ pointed out that anions drag up to four water molecules into the organic phase throughout partitioning of quaternary amine salts between water and nitrobenzene. No dragged water was found upon the entrance of the QA cation. Thus, in the presence of ions, an excess water fraction was expected to appear as compared to the 1:208 molar ratio for the water-saturated dichloromethane. Our computational possibilities allowed consideration of a DCM box with 250–255 solvent molecules. By adding 2 water molecules to the system, the excess water concentration was assured (the water:DCM molecular ratio is about 1:127, nearly double the ratio of 1:208 for the saturated solution). In the partition experiments the concentration of the organic solute was in the order of magnitude of 10^{-5} . It was impossible to model such dilute solutions. Thus a compromise had to be made in developing our computer model: the dichloromethane solvent contains a reasonable amount of excess water, and the system is as dilute for the organic ion-pair as is technically possible.

Ion-Pair Structure in Solution. The TIP4P water in an aqueous environment was studied first by Jorgensen et al.²³ The maximum of the O···O radial distribution function was found at about 2.8 Å at $T = 298$ °C. Mezei and Ben Naim³⁹ calculated the potential of mean force between two water molecules placed in liquid water in several fixed relative orientations when no hydrogen bond formation was possible within the dimer. Minima for the PMFs, without considering the solute–solute interaction energy, were found at O···O separations of at least 3.2 Å.

Figure 2 shows the PMF for the water dimer in DCM. Assigning the $dG = 0$ value to an arbitrary O···O distance, the PMF shows the changes in the solvation free energy when increasing the water···water separation. The curve shows its minimum at $R(O···O) = 2.8$ Å, and reaches a nearly constant value after $R = 3.8$ Å. The PMF indicates that the two water molecules form a dimer at a distance allowing hydrogen bond formation. For disrupting this bond and separating the oxygen atoms as much as about 3.8 Å, the activation free energy is 3.2 kcal/mol at $T = 298$ °C. A second minimum with stabilization free energy of 0.1–0.2 kcal/mol appears at $R = 7.5$ Å. Considering, however, the 0.07 kcal/mol standard deviation for

(35) DeBolt, S. E.; Kollman, P. A. *J. Am. Chem. Soc.* **1995**, *117*, 5316.

(36) Best, S. A.; Merz, K. M., Jr.; Reynolds, C. H. *J. Phys. Chem. B* **1999**, *103*, 714.

(37) Dang, L. X. *J. Chem. Phys.* **1999**, *110*, 10113.

(38) Osakai, T.; Ogata, A.; Ebina, K. *J. Phys. Chem. B* **1997**, *101*, 8341.

(39) Mezei, M.; Ben-Naim, A. *J. Chem. Phys.* **1990**, *92*, 1359.

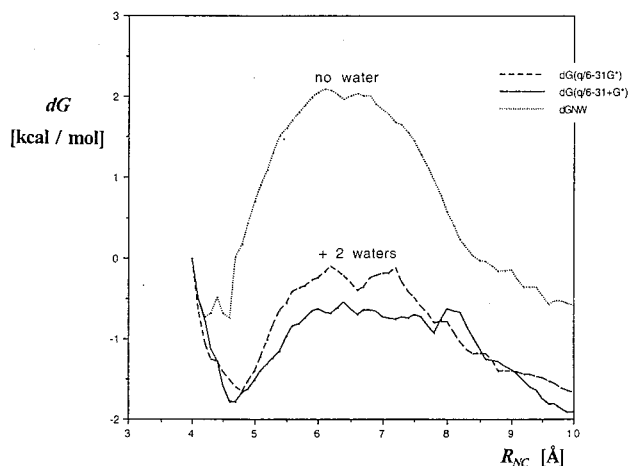


Figure 3. PMF for trimethylaniline–acetate in DCM. Codes in parentheses refer to the ab initio basis set used in charge determination. Abbreviation NW stands for system with no water.

the calculated -0.21 kcal/mol free energy change in the range of 5.2 – 7.4 Å, the minimum may not have real physical relevance. MD results of Dang³⁷ predict a relatively narrow liquid/liquid interface between water and dichloromethane. If, however, the two phases are separated and the water-saturated dichloromethane is to be studied, then the calculated PMF profile suggests that water molecules do not dissolve favorably in DCM, and probably form dimers or even larger water clusters.

Figure 3 contains the PMFs for the trimethylaniline–acetate (TMA/AC) system. Two different types of calculations have been carried out. The lower two curves were obtained when the ion-pair and two water molecules set up the solute system. Using HF/6-31G* and HF/6-31+G* electrostatic potential fitted atomic charges for the acetate ion, the two curves run very similarly. O and carboxylate C atomic charges of -0.7 and 0.9 , respectively, change to -0.8 and 1.1 upon adding the diffuse functions to the atomic basis set in the ab initio calculations. The PMFs have their first minima in the range of $R(N\cdots C) = 4.6$ – 4.9 Å, indicating a contact ion-pair here. There is a sustained maximum between about 6 and 7 Å, and both curves decrease at larger $N\cdots C$ separations. The activation free energy for the ion separation is 1.2 – 1.5 kcal/mol based on the two curves.

The course is qualitatively similar for the third PMF obtained without two water molecules in the system. HF/6-31G* derived atomic charges were used in this simulation, thus dotted and dashed line curves are to be compared. In the absence of water molecules the $N\cdots C$ separation in the contact ion-pair is obviously shorter by about 0.3 – 0.5 Å. This is well explained by considering that snapshots unanimously showed each water molecule forms a stable hydrogen bond to the carboxylate group. This structure is characteristic for the anion $\cdots 2$ water system not only for the acetate ion, but for all anions considered here in the DCM simulations. As a consequence, the stable trimer cannot get as close to the cationic head as the simple anion can. The stronger ion–ion interaction explains then that activation free energy for ion-pair separation is larger by about 1 kcal/mol without rather than with water in the system. The free energy of the system is at maximum in the range of $R(N\cdots C) = 6$ – 7 Å, and the curve sinks at larger separations.

All three curves indicate at least another minimum in the separate ion-pair range, $R(N\cdots C) > 10$ Å. This modeling-predicted second minimum may be, however, artificial if considering the cutoff procedure more closely. The solute–solvent cutoff radius was set to 15 Å. When the $N\cdots C$ separation

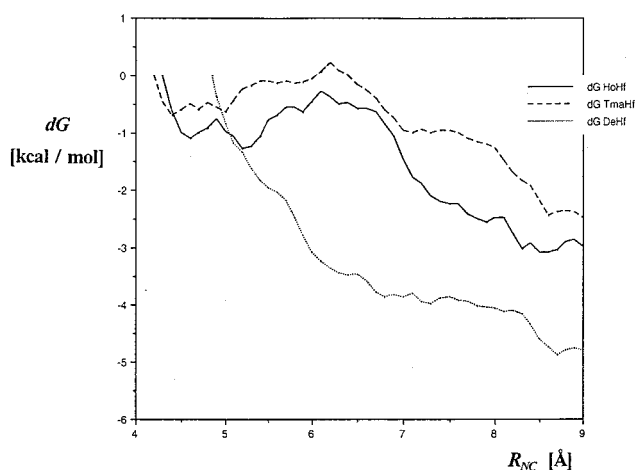


Figure 4. PMF for homidium–Hfumarate (HoHf), trimethylaniline–Hfumarate (TmaHf), and *N*-methyl deramcyclyne–Hfumarate (DeHf) in DCM.

increases, more and more solvent molecules will be explicitly considered in the solute–solvent interaction. This may be of small importance with a neutral solute, as in the case of the water dimer. Considerably more negative interaction energy may be calculated, however, if ionic solutes interact with a solvent of dipole moment 2.38 D, as happens when the three-point model of DCM is applied.²²

Three remarkably different PMFs are compared in Figure 4. All three ion-pairs have the hydrogen fumarate ion as their anion, thus differences reflect the cation effect on the PMF. With the smallest TMA cation the contact arrangement is locally stable in the $R(N\cdots C)$ range of 4.4 – 5.0 Å. The activation free energy is about 0.7 kcal/mol. There is a shoulder at $R(N\cdots C) = 7$ Å, and the calculated lowest relative free energy at $R(N\cdots C) = 8.8$ – 9.0 Å indicates the preference for a solvent-separated ion-pair arrangement. The trend is more pronounced with the larger homidium ion: there is a well-defined double-minimum of the PMF in the contact ion-pair separation range of $R(N\cdots C) = 4.5$ – 5.5 Å and the potential curve decreases after $R(N\cdots C) = 7$ Å. An explanation for the double minimum (also seen for the TMA-HFUM ion-pair) is difficult. It is considered as an indication for orientational effects that the $N\cdots C$ distance is not the single determinant of the interaction energy for a bulky ion with delocalized charge distribution. The unit positive charge is localized in 61% on the $N(\text{CH}_3)_3$ group in TMA, but only in 55% on the $\text{CN}(\text{CH}_2)\text{C}$ moiety in HOM. Because of the extension of the ions, different orientations with hardly different $N\cdots C$ separations can cause some tenths of a kcal/mol difference in the solvation free energy in the contact ion-pair range. (Figure 6 shows rapid changes in E_{XX} and E_{SX} for the HOM-HFUM ion-pair in the $R(N\cdots C)$ range of 5.0 – 5.7 Å.) The solvent-separated ion-pair seems to be stabilized at about $R(N\cdots C) = 8.5$ Å, and the activation free energy for the separation is about 1 kcal/mol.

MeDER has a charge localization of 73% at the $N(\text{CH}_3)_3$ cationic head. It is surprising that not even the locally stable contact ion-pair has been found for the MeDER-HFUM system allowing the most concentrated charge–charge interaction of the three pairs compared here. The PMF decreases almost monotonically. It has a shoulder at about $R(N\cdots C) = 7$ Å, but stabilization for the ion-pair was calculated only at around 9 Å. Since, however, the PMF has not been calculated beyond this separation, its further decrease may not be ruled out. Indeed, for structures such as MeDER with considerable decrease of free energy in the 5 – 9 Å range, further free energy decrease is

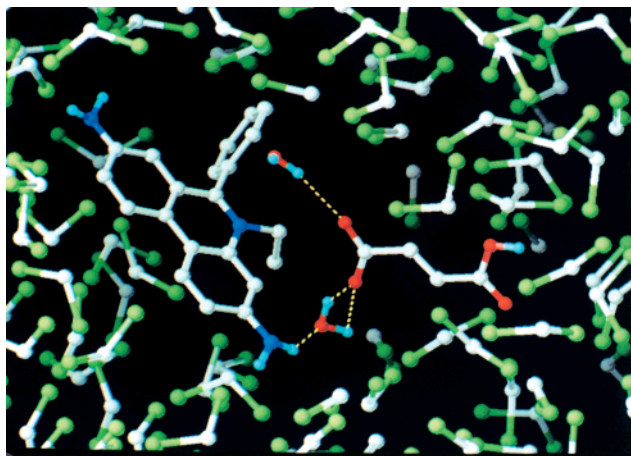


Figure 5. Snapshot after taking 5000K configurations in the averaging phase of the Monte-Carlo simulations for the contact homidium–Hfumarate (HOM-HFUM) ion-pair + 2 water molecules in DCM. $R(N\cdots C) = 4.40 \text{ \AA}$.

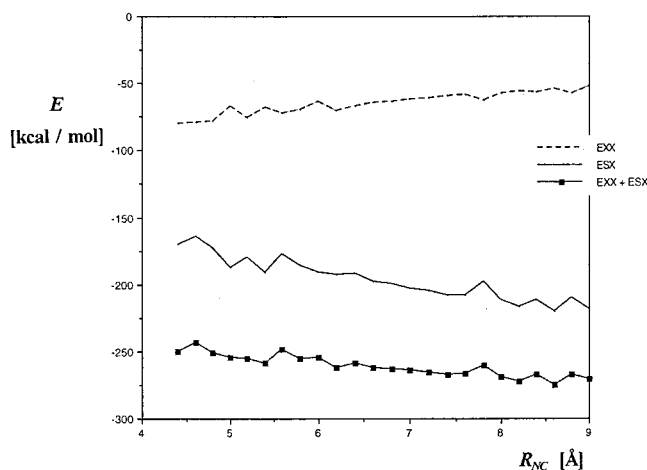


Figure 6. Solvation energy terms for the homidium–Hfumarate ion-pair in DCM. E_{XX} and E_{SX} stand for the solute–solute and solute–solvent interaction energies, respectively. $E_{XX} + E_{SX}$ gives the total solvation energy, E_{tot} .

still possible, leading to almost “free” ions in a water-saturated polar organic solvent.

While PMFs are similar in shape for the TMA and HOM cations that are different in size, the HOM and MeDER ions, closer in size, produce qualitatively different PMFs. These results suggest that neither the size nor the charge localization determines exclusively the behavior of an ion-pair in dichloromethane. The PMFs indicate that contact ion-pairs are possible in DCM but they have been calculated to be less stable than the solvent-separated arrangement by about 2 kcal/mol. The activation free energy of ion separation is small, about 1 kcal/mol at $T = 298 \text{ }^\circ\text{C}$, thus equilibration of the different arrangements is possible. Furthermore, the existence of largely separated, nearly free ions should also be taken into consideration when characterizing the equilibrium mixture. In their MD simulations for dilute solutions of NaI in dimethyl ether, Payne et al.⁴⁰ found about 44% contact ion-pairs and about 22% free ions.

Figure 5 shows a snapshot taken at the end of Monte-Carlo simulations for the HOM-HFUM ion-pair at $R(N\cdots C) = 4.40 \text{ \AA}$. There is a hydrogen bond network involving the 8-NH₂

group, one of the water molecules, and the carboxylate group. Such a network is possible only at small ion-pair separation and may certify the locally stable contact ion-pair arrangement. No such hydrogen bond network has been found with the other two cations.

The only acceptor site in the MeDER ion is the ether oxygen. Snapshots have not shown interaction with either water hydrogens or the neutral carboxyl in HFUM. Involvement of the carboxylic OH in a hydrogen bond would require an almost parallel arrangement of the anion and the side chain. No such orientation of the anion has been found characteristic in the equilibrium structure. In contrast, favorable interaction of the ionic heads is possible in TMA-HFUM, while a water hydrogen forms an H-bond with the benzene ring. The water–benzene π -hydrogen bond has been pointed out to be of remarkable stability.⁴¹ In conclusion, hydrogen bonds possible within the ion-pair and/or small hydrates thereof may be an important factor for stabilizing the contact form as compared to the solvent separated one.

Snapshots also show that the $N(\text{cation})\cdots C(\text{anion})$ axis is generally nearly collinear with the main axis of the rodlike anions in the equilibrium arrangements. The main axis is the $C_1\cdots C_4$ axis for the HFUM anion and the $S\cdots C(\text{methyl})$ axis of the PTS anion. Comparison of the DCM/water data in Table 1 indicates the importance of the length of the rodlike anion for the HOM-containing ion-pairs. The $S\cdots C(\text{methyl})$ and $C_1\cdots C_4$ distances were calculated at 6.12 and 3.91 \AA , respectively, from ab initio geometry optimizations. The average length of the CPR (caproate) anion was calculated by performing molecular mechanics conformational analysis in chloroform, the low polarity solvent available in the MacroModel 6.5 modeling package.⁴² Modeling showed that at least one trans conformation along the $C_1\cdots C_6$ pathway is required for obtaining a low-energy conformer. The lowest energy ggg form was found higher in energy by 2.7 kcal/mol than the tgt conformer, most stable in chloroform. The four lowest energy structures, tgt, ttt, ttg, and tgg (within the enthalpy range of 0.64 kcal/mol at $T = 298 \text{ }^\circ\text{C}$), were considered to estimate the Boltzmann average of the $C_1\cdots C_6$ distance as $R = 5.79 \text{ \AA}$. Taking the “rod-length” for PTS, CPR, and HFUM, a linear dependence of $\log P'$ on the R values was found for these three ions. This result suggests that theoretically determined geometric parameters may be useful in predicting relative $\log P'$ values. The importance of the geometric aspects was recently confirmed by finding good linear correlation between octanol/water $\log P'$ and the water accessible surface area of the organic anion in salts with quaternary ammonium cations.¹⁸

The solute models above contained not only the ion-pair but also two water molecules. $H_w\cdots O(\text{carb})$ distances in hydrogen bonds to the carboxylate group were found frequently as short as 1.7 \AA . The $O_w H_w\cdots O(\text{carb})$ angles were generally at least 150° . Such $\text{HOH}\cdots\text{OCO}\cdots\text{HOH}$ geometry, maintained most of the time, prevents water molecules of forming hydrogen bonds with each other. Thus two nearly linear hydrogen bonds to the carboxylate group is superior as compared to a ring system with three, strongly bent hydrogen bonds including that between the waters. This finding indicates a different structure for some water molecules when penetrating into the water/dichloromethane interface or when forming a strong hydrogen-bonded hydrate with the anion.

(41) (a) Suzuki, S.; Green, P. G.; Bumgarner, R. E.; Dasgupta, S.; Goddard, W. A., III; Blake, G. A. *Science* **1992**, 257, 942. (b) Augspurger, J. D.; Dykstra, C. E.; Zwier, T. S. *J. Phys. Chem.* **1993**, 97, 980.

(42) *MacroModel 6.5*, Mohamdi, F.; Richards, N. G. J.; Guiga, W. C.; Liskamp, R.; Lipton, M.; Caufield, C.; Chang, G.; Hendrickson, T.; Still, W. C. *J. Comput. Chem.* **1990**, 11, 440.

(40) Payne, V. A.; Xu, J.-H.; Forsyth, M.; Ratner, M. A.; Shriver, D. F.; De Leeuw, S. W. *J. Chem. Phys.* **1995**, 103, 8734, 8746.

In some percents of the configurations (mainly at short N \cdots C distances), one of the water molecules hydrated the neutral COOH group of HFUM. The back and forth motion of one water molecule may indicate the difficulty for favorably accommodating a second water molecule in the contact ion-pair region. In combination with the possible orientational effect, subtle structural changes may result in development of two close minima of the PMF. Although this effect is almost equally available both for the MeDER and TMA cations, the considerable difference in the size and shape of the hydrophobic site may provide an explanation.

Energy terms for the solutes with close ion-pair elements or separated by the solvent are summarized in Table 2a,b. The BOSS program makes it possible to calculate total energy terms and energy terms for a specified single solute, as well. In our study the cation was selected as the special ion and distinguished with superscript 1. Thus, E_{XX}^1 indicates the solute–solute interaction between the cation (ion 1) and other solutes (anion + 2 waters) in DCM. E_{XX} is the total solute–solute interaction energy and $E_{XX} - E_{XX}^1$ accounts for the interaction energy among the three other solutes.

The tables show that the $E_{XX} - E_{XX}^1$ energy term is nearly constant for any ion-pairs when comparing the values at short and large R values. This is strong support for the above qualitative statement, that the structure (and interaction energy) in the water \cdots anion \cdots water trimer is fairly constant. Three of the four ion-pairs in Tables 2 refer to Hfumarate salts, thus one may expect equal $E_{XX} - E_{XX}^1$ values at large R . The energy values vary within a 3 kcal/mol range, indicating that the cation still has an effect on the interaction energy of the trimer even at larger separations.

The trimer behaves nearly as a point charge at large R . The $E_{XX}^1(C)$ Coulomb term fits nicely to the $1/R$ function when considering the values at $R = 8.9, 9.0, 9.8$ Å with the HFUM anion. Furthermore, the $E_{XX}^1(C)$ energy shows a very good $1/R$ fit for the HOM-PTS system at 5.25 and 9.90 Å separations. These results confirm the idea about the stability of the water \cdots anion \cdots water structure for a given anion. (The value of $E_{XX}^1(C)$ itself depends, of course, on the chemical constitution of the ion-pair.)

The Lennard-Jones (LJ) components of the E^1 terms are of small absolute value for the X–X interactions even at the contact ion-pair region. In contrast, the solvation energy $E_{SX}^1(LJ)$ term is a large negative value depending mostly on the cation size. It is -20 kcal/mol for the smaller TMA cation and -45 kcal/mol for the bulky HOM cation with the contact ion-pair. The term becomes only moderately more negative at larger ion-pair separations. Solvent molecules with remarkable contribution to the $E_{SX}^1(LJ)$ term cover the larger part of the cation surface, not facing the anion, already in the contact form. Changes in $E_{SX}^1(LJ)$ up to 5 kcal/mol at larger separations indicate interactions with some new solvent molecules replacing the anion on the former contact surface. The energy change is relatively small: only close solvent molecules have remarkable contributions to $E_{SX}^1(LJ)$, due to the R^{-6} distance dependence of dispersion energy in the OPLS potential. The $E_{SX}^1(C)$ term also becomes more negative at larger ion separation allowing the appearance of more solute molecules around the solute. The energy decrease is more pronounced here, however, due to the only $1/R$ decay of the charge–charge interaction.

The courses of the curves for the solvation energy components (Figure 6) are typical for all ion-pairs above. The solute–solute interaction energy, E_{XX} , becomes less negative with increasing N \cdots C separation, in compliance with the Coulomb law. The

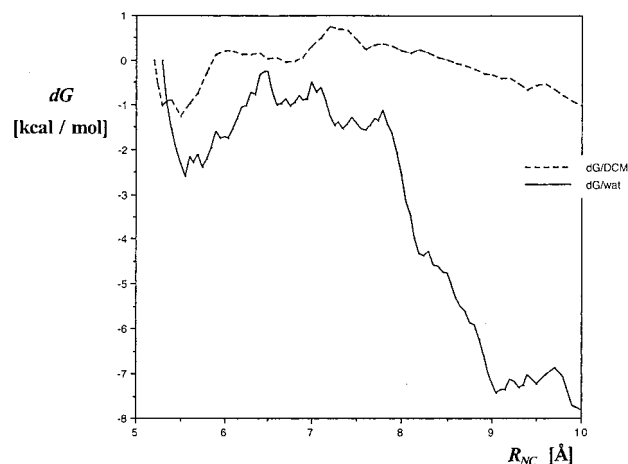


Figure 7. PMF for the homidium–*p*-toluene sulfonate ion-pair in DCM and water.

solute–solvent energy, E_{SX} , decreases in the same transformation. The course of E_{tot} ($=E_{XX} + E_{SX}$) reflects the dominant term, which is the solute–solvent interaction energy in all cases studied here. The opposite course of E_{XX} and E_{SX} is maintained not only globally but also locally, as seen from the compensating effect in the range of 4.8–5.5 Å and at $R = 7.8$ Å.

The solvent effect on PMF is shown in Figure 7. The HOM-PTS ion-pair plus two water molecules were studied in DCM, and the ion-pair itself was investigated in aqueous solution. (C is the ring carbon in the $R(N\cdots C)$ distance, thus Figures 4 and 7 are not directly comparable.) Both curves in Figure 7 show a locally stable contact ion-pair arrangement. There is a very shallow, higher lying second minimum in DCM at about 7 Å. The separated ion-pair at 10 Å is approximately as stable as the contact pair at 5.5 Å. The barrier between the two arrangements is about 2 kcal/mol.

The PMF in water is much different. The contact ion-pair is stable at $R = 5.6$ – 5.8 Å. There is a 2 kcal/mol barrier and a vague stabilization around $R = 7$ Å, as is also found in DCM, but then the PMF steeply decreases in the $R = 8$ – 9 Å range. The separated ion-pair is stabilized (at least locally) in the range $R = 9$ – 10 Å. Overall, the separated HOM-PTS ion-pair is more stable than the contact one by 5 kcal/mol, in contrast to the nearly equal free energy in DCM.

Solute Hydration. (a) Hydration of the Aniline-Type NH₂ Group. Monte-Carlo simulations provide an insight into the hydration-shell structure of polar groups. In a series of calculations many N-containing compounds have been studied in this respect: primary^{43,44} and secondary⁴⁴ amines, pyrrole,⁴⁵ imidazole,⁴⁵ pyridine derivatives,⁴⁶ and the protonated aliphatic NH₂ group in histamine⁴⁷ and dopamine.⁴⁸ The homidium ion contains the aniline-type NH₂ group, which will be more closely studied in this section.

Table 3 shows the geometric and atomic charge parameters for some NH₂-containing molecules. Atomic charges for the four NH₂ groups are remarkably different. The $q(\text{NH}_2)$ group charges are almost identical for the homidium ion, but they differ considerably from those for methylamine and the neutral aniline.

(43) Dunn, W. J., III; Nagy, P. I. *J. Phys. Chem.* **1990**, *94*, 2099.

(44) Dunn, W. J., III; Nagy, P. I. *J. Comput. Chem.* **1992**, *13*, 468.

(45) Nagy, P. I.; Durant, G. J.; Smith, D. A. *J. Am. Chem. Soc.* **1993**, *115*, 2912.

(46) Nagy, P. I.; Takács-Novák, K. *J. Am. Chem. Soc.* **1997**, *119*, 4999.

(47) Nagy, P. I.; Durant, G. J.; Hoss, W. P.; Smith, D. A. *J. Am. Chem. Soc.* **1994**, *116*, 4899.

(48) Nagy, P. I.; Alagona, G.; Ghio, C. *J. Am. Chem. Soc.* **1999**, *121*, 4804.

Table 2. Energy Components for the Ion-pair Interactions in Dichloromethane^a

(a) Homidium...A ⁻				
A ⁻	Hfumarate		<i>p</i> -toluenesulfonate	
$R(N\cdots C)/\text{\AA}$	4.40	9.00	5.25	9.90
E_{XX}^1 (C)	-54.2(3)	-30.0(2)	-65.5(3)	-34.7(3)
E_{XX}^1 (LJ)	-2.8(1)	-0.4(0)	-7.4(1)	-0.4(0)
E_{SX}^1 (C)	-26.6(5)	-44.3(5)	-11.1(5)	-38.7(5)
E_{SX}^1 (LJ)	-44.7(2)	-48.5(2)	-43.0(2)	-48.3(2)
E_{XX}	-79.9(4)	-52.7(3)	-97.7(2)	-59.9(4)
$E_{XX} - E_{XX}^1$	-22.9(5)	-22.3(4)	-24.8(4)	-24.8(5)
E_{SX}	-170.5(6)	-218.3(11)	-131.1(9)	-201.4(10)
$E_{SX} - E_{SX}^1$	-99.2(8)	-125.5(12)	-77.0(11)	-114.4(11)

(b) B ⁺ ...Hfumarate				
B ⁺	trimethylaniline		<i>N</i> -methylderamcyclane	
$R(N\cdots C)/\text{\AA}$	4.30	8.90	4.90	9.80
E_{XX}^1 (C)	-60.8(2)	-30.8(2)	-50.0(3)	-27.8(2)
E_{XX}^1 (LJ)	-2.0(1)	-0.1(0)	-0.2(1)	-0.1(0)
E_{SX}^1 (C)	-25.5(6)	-51.8(5)	-32.7(4)	-52.8(4)
E_{SX}^1 (LJ)	-20.2(1)	-21.5(1)	-39.5(1)	-41.3(2)
E_{XX}	-87.8(2)	-56.3(2)	-73.8(5)	-50.1(4)
$E_{XX} - E_{XX}^1$	-25.0(3)	-25.4(3)	-23.6(6)	-22.2(4)
E_{SX}	-139.2(9)	-195.0(11)	-177.1(6)	-223.3(10)
$E_{SX} - E_{SX}^1$	-93.5(11)	-121.7(12)	-104.9(7)	-129.2(11)

^a Energies in kcal/mol. Superscript 1 refers to the cation. Subscripts XX and SX stand for the solute-solute and solvent-solute energy terms, respectively. Letters C and LJ refer to the Coulomb and Lennard-Jones energy terms, respectively. Values in parentheses stand for the standard deviations in the unit of the last decimal.

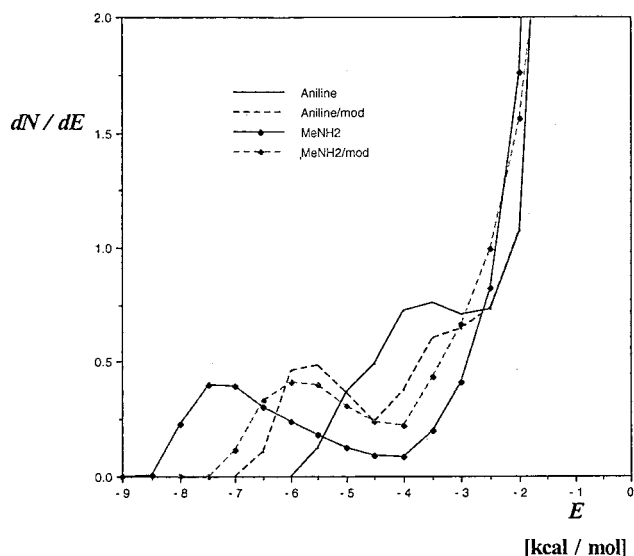
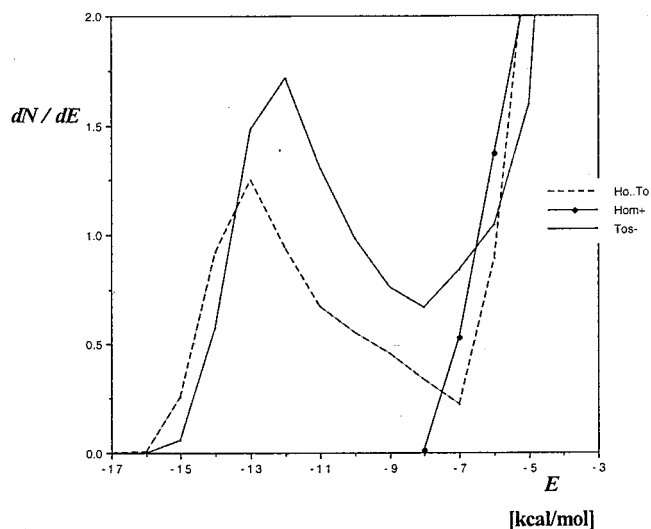
Table 3. Geometric and Charge Parameters for the NH₂ and SO₃⁻ Groups in Different Molecules^a

	MeNH ₂	aniline	homidium	
			N ₈	N ₃
C-N	1.453	1.397	1.381	1.367
N-H	1.001	0.997	0.997, 0.996	0.995, 0.995
CNH	110.66	114.29	116.41, 116.35	118.10, 118.61
HNH	106.86	110.69	112.20	114.08
$q(N)$	-1.040	-0.946	-0.957	-1.001
$q(H)$	0.374	0.368	0.386, 0.417	0.418, 0.423
$q(NH_2)$	-0.291	-0.209	-0.155	-0.160

<i>p</i> -toluene sulfonate	
S-C	1.797
S-O	1.454, 1.453, 1.453
OSO	113.64, 113.93, 114.41
OSCC	78.12, -41.46, -161.90
$q(S)$	1.577
$q(O)$	-0.808, -0.806, -0.800
$q(SO_3^-)$	-0.836

^a Geometries optimized at the HF/6-31G* and HF/6-31+G* levels for NH₂ and SO₃⁻ groups, respectively. Atomic charge parameters for the Monte-Carlo simulations were obtained with the CHELPG procedure²⁸ fitting atomic charges to the corresponding molecular electrostatic potentials.

Methylamine- and aniline (solute)-water (solvent) pair-energy distributions are compared in Figure 8. The $(dN/dE)\Delta E$ product taken at E gives the number of the solvent (water) molecules in the interaction energy of $E \pm 0.5\Delta E$ with the solute. In a numerical determination of the pair-energy distribution function ΔE was taken at 0.5 and 1 kcal/mol for the curves indicated in Figures 8 and 9, respectively. Solid lines in Figure 8 were obtained with the atomic charges in Table 3. Dotted line curves were obtained when the corresponding N and H atomic charges of the two molecules were switched, and the

**Figure 8.** Pair-energy distribution functions for aniline and methylamine in water. Extension "mod" indicates methylamine charges for aniline (aniline/mod) and aniline charges for methylamine (MeNH₂/mod).**Figure 9.** Pair-energy distribution functions for the contact homidium-*p*-toluene sulfonate ion-pair (HoTo), the homidium ion (Hom⁺), and the *p*-toluene sulfonate ion (Tos⁻) in water.

resulting change in the net molecular charge was corrected at the connecting C atom.

Pair-energy distribution functions typically show a double-maximum course with polar solute in water. The high peak (cut here in Figures 8 and 9) at $E = 0$ indicates that the solute-solvent interaction energy is close to zero for most solvent molecules. The maximum in the negative E range is due to solvent molecules in distinguished, stabilizing interaction with the solute. Previous results^{23,43-49} indicate that integration of the dN/dE curve until its first minimum provides a reasonable estimate for the number of the solute-solvent hydrogen bonds, n_{HB} .

Aniline charges in methylamine result in a shift of the maximum toward higher energies. The minimum, however, stays at $E = -4$ kcal/mol, and integration until this limit confirms our previous findings:^{43,44,47} the calculated number of the hydrogen bonds, $n_{HB} \sim 1$, for methylamine is rather insensitive to small changes in the molecular geometry and potential function parameters.

(49) (a) Jorgensen, W. L.; Madura, J. D. *J. Am. Chem. Soc.* **1983**, *105*, 1407. (b) Jorgensen, W. L.; Swenson, C. J. *J. Am. Chem. Soc.* **1985**, *107*, 1489.

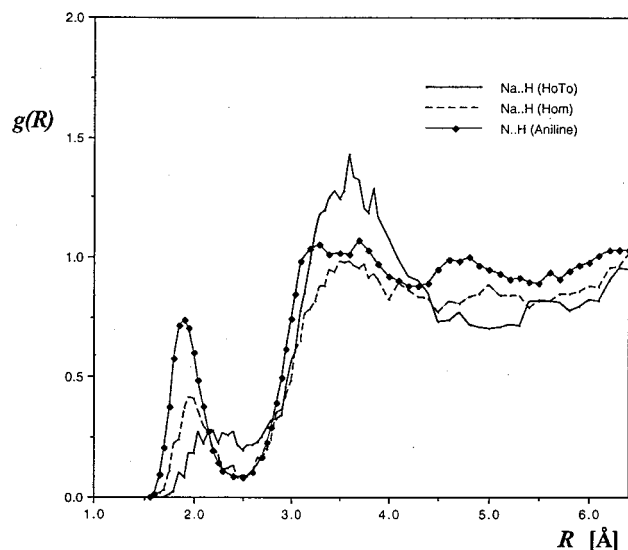


Figure 10. N...H(water) radial distribution functions for aniline type nitrogens in the contact homidium-*p*-toluene sulfonate ion-pair (HoTo), the homidium ion (Hom⁺), and neutral aniline.

Aniline shows larger sensitivity to changes in the charge parameters. The fitted, "true" parameters (unmarked solid line) result in a distribution curve starting at $E = -6$ kcal/mol, having a shoulder in the energy range of -5 and -4.5 kcal/mol, and a maximum and a minimum at $E = -3.5$ and -3.0 kcal/mol, respectively. The curve starts rapidly increasing at $E = -2.5$ kcal/mol. The integral up to $E = -4.5$ (the end of the shoulder) indicates 0.5 water molecules in some type of hydrogen bond. A further 1.5 molecules were obtained involved in another type of hydrogen bond calculated from integration until $E = -2.5$ kcal/mol.

When methylamine parameters are used for aniline (dashed line) the maximum of the curve moves toward lower energies. Since the modified parameters increase the net negative charge on the nitrogen atom, this modification corresponds to formation of a more basic nitrogen. Thus the shoulder on the true curve has been identified as referring to the hydrogen bond to water with nitrogen atom as the acceptor in aniline. The calculated number of aniline N...H-O bonds is 0.5, as obtained from the true curve. This number is considerably smaller than 1 obtained for methylamine, and is in line with the experience that aniline is much less basic than methylamine.

Pair-energy distribution for the homidium ion is shown in Figure 9. It starts at $E = -8$ kcal/mol and increases steeply. It does not show the curve characteristics obtained for aniline: there are 2 water molecules in the energy range of -8 and -6 kcal/mol, and a further 14 in the $E = -6$ to -3 kcal/mol range. Four water molecules expected to be bound to the two amino groups are probably included in the calculated 14 solvent molecules.

The existence of an aniline N...H-O hydrogen bond may also be concluded upon inspection of radial distribution functions. Figure 10 shows the N...H(water) rdfs for aniline, the homidium ion, and the homidium-*p*-toluene sulfonate ion-pair at the minimum free-energy contact ion-pair arrangement ($R = 5.55$ Å, Figure 4). Aniline shows a well-defined peak on $g(R)$ at $R = 1.90$ Å. The peak is slightly shifted upward for the homidium ion, but more importantly, the peak value is about half of that for aniline. This indicates weaker localization of water hydrogens in positions favorable for the N...H-O bond formation. The finding is reasonable: although the nitrogen atomic charge, -1.001 , is slightly more negative than that for

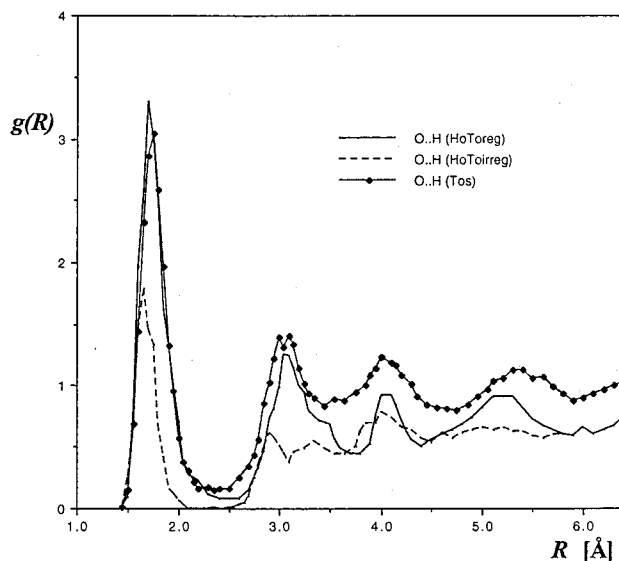


Figure 11. O...H(water) radial distribution functions for the *p*-toluene sulfonate ion with regular oxygen (HoToreg) and irregular oxygen (HoToirreg) in the contact homidium-*p*-toluene sulfonate ion-pair, and the *p*-toluene sulfonate ion (Tos⁻).

aniline, the overall positive charge of the cation may disfavor the location of a water hydrogen of positive atomic charge at the amine site. Reduced peak value and broadened $g(R)$ for the HOM-PTS ion-pair is, however, surprising. One may expect an increase instead of a decrease of the $g(R)$ peak value, as compared to the curve for the positive ion. An added negative ion (ion-pair vs single cation) should make the electrostatic potential more negative at the site where the hydrogen bond is to be formed. Accordingly, increased preference for hydrogen location and, consequently, higher $g(R)$ peak were expected. An explanation for the opposite computational results will be given in the next section discussing the hydration of the PTS ion.

(b) Hydration of the *p*-Toluene Sulfonate Ion. The number of hydrogen bonds to the PTS anion was calculated at 7.6 upon integration of the PTS-water pair-energy distribution function until its minimum at $E = -8$ kcal/mol (Figure 9; in Figures 9–12 the *p*-toluene sulfonate ion is referred to as tosylate and abbreviated as Tos, the homidium-PTS ion-pair as homidium-tosylate, HoTo). One of the three similar H(water)...O(PTS) rdfs is shown in Figure 11 (marked line). There is a high first peak at $R(\text{H}\cdots\text{O}) = 1.75$ Å, and three additional peaks at larger R values. The well-resolved maximum–minimum character of the $g(R)$ function indicates a strongly localized water structure around the ionic site. Integration of the three H...O rdfs up to the corresponding first minima gives O/H coordination numbers of 2.6, 2.3, and 2.8. Thus, there are altogether 7.7 hydrogens close to the oxygen atoms. On the basis of the calculated value of 7.6 for the water-PTS hydrogen bonds, almost all these close hydrogens are involved in bond formation.

The S...O(water) rdf (not indicated) starts at $R = 3.05$ Å. Its first maximum and minimum are at $R = 3.80$ and 4.35 Å, respectively. Integration until this minimum gives 9.3 water oxygens around the sulfur atom. It is a slightly larger value than the sum of the O/O(water) coordination numbers, $2.8 + 2.4 + 2.9 = 8.1$, calculated from the integration of the corresponding rdfs until their first minima. The difference reflects the larger $R(\text{min})$ value of 4.35 Å applied in the S/O(water) calculations as compared to $R(\text{min}) = 3.15$ – 3.20 Å used in calculating the O/O(water) coordination numbers. Since the S–O distance is 1.45 Å, the sulfur atom "sees" almost

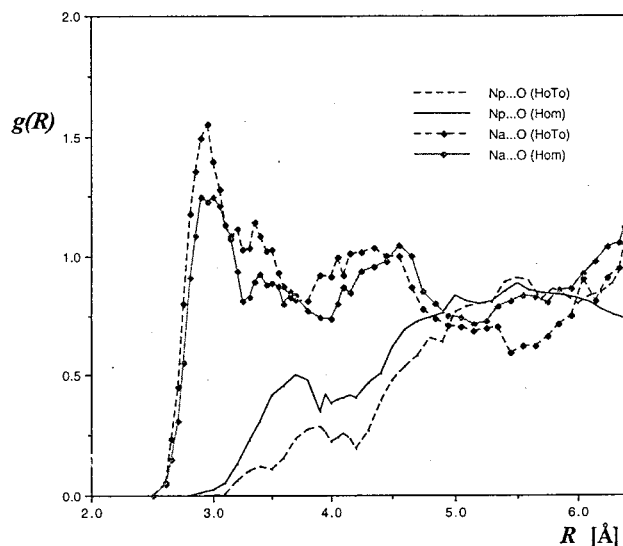


Figure 12. N...O(water) radial distribution functions for pyridine type (Np) and aniline type (Na) nitrogens in the contact homidium-*p*-toluene sulfonate ion-pair (HoTo) and in the homidium ion (Hom⁺).

all water molecules seen by the PTS oxygens, but the S/O(water) coordination number has also contributions from waters hydrating the aromatic ring.

If considering, however, the O...H rdf's for the HOM-PTS ion-pair, one regular and two irregular (only one of them is shown) rdf's were obtained. Locations of maxima and minima, and the $g(R)$ peak value for the regular rdf are close to those calculated for the pure anion in water. For the irregular HoTo rdf, however, all corresponding $g(R)$ values are only about half of the PTS rdf values. This result indicates a serious deficiency of close water molecules and hydrogen bonds for 1 or 2 oxygens of the SO_3^- group. Integration of the pair-energy distribution function until $E = -7$ kcal/mol (Figure 9) gives the calculated number of hydrogen bonds as 5.6, showing a loss of two hydrogen bonds as compared to the free anion. The O/H(water) coordination number, based on integration of rdf's, is $2.7 + 1.0 + 2.1 = 5.8$. Thus about two water molecules have been repelled from the hydration sphere of the anion, due to steric repulsion emerging at the formation of a contact ion-pair. The determined small difference between the O/H(water) coordination number and the number of hydrogen bonds, 5.8 vs 5.6, suggests that most of the close water hydrogens are still involved in hydrogen bonds.

Figure 12 shows the N...O(water) rdf's for both types of nitrogen atoms, both in the pure homidium ion and the contact HOM-PTS ion-pair. The unmarked curves indicate only a weak stabilization of the water oxygens around the pyridinium nitrogen at N...O distances of about 4 Å. It is noteworthy that the Np...O rdf has a remarkably smaller peak value in the presence of the PTS counterion than with the pure homidium ion. Snapshots clearly indicate that there is no room for accommodating even one water molecule between the pyridinium nitrogen and the $-\text{SO}_3^-$ group in the contact ion-pair arrangement. The N-CH₂-CH₃ plane is almost perpendicular to the plane of the condensed aromatic ring (regarded as the general plane of the homidium cation). Interaction with the PTS ion is feasible if the anion is located in the half-space opposite to that containing the ethyl group. In this arrangement, however, the pyridinium nitrogen cannot be remarkably solvated by waters because of steric hindrance in both half-spaces. One half-space

is opened for hydration for the pure homidium ion, and this structural change is reflected in the corresponding Np...O(water) rdf.

The presence of a contact PTS ion shows an effect on the N(aniline)...O(water) rdf as well. In this case, however, the close PTS increases, rather than decreases, the peak value of the $g(R)$ curve. The maximum $g(R)$ values are 1.50 and 1.25 for the ion-pair and the pure homidium ion, at a N...O distance of about 2.95 Å. In summary, the contact PTS counterion decreases the hydration of the pyridinium nitrogen of the homidium ion, increases the water oxygen local concentration about the aniline nitrogen, but decreases the local water hydrogen concentration about the same nitrogen (see previous section). These findings altogether can be consistently explained by also considering the water deficiency around the SO_3^- site in the contact ion-pair. The system tries to enhance its stability reduced upon repelling about two water molecules throughout the ion-pair formation. The anion increases the local water concentration at all possible sites around the PTS. The space is crowded around the pyridinium nitrogen, but there is no steric hindrance around the NH₂. The water molecules are strongly localized in these regions, but the water hydrogens, due to strong electrostatic interaction with it, point toward the PTS anion. As a consequence, the water hydrogens generally cannot form an N...H-O hydrogen bond with the aniline nitrogens. Water H's are strongly localized, but in an unfavorable position for hydrogen bond formation. Indeed, Figure 10 shows an outstanding N...H peak for the HoTo dimer at a N...H separation of 3.6 Å, completing the argument about the role of the contact *p*-toluene sulfonate counterion.

Model for Ion-Pair Partition. Dang pointed out recently⁵⁰ that *separate* transfers of a Cs⁺ and a Cl⁻ ion from water into the bulk CCl₄ require 19 and 17 kcal/mol, respectively. The average dipole moment for the bulk dichloromethane was calculated at 1.9 D,³⁷ which indicates a fairly polar solvent as compared to CCl₄. Thus, the free energy of even the separate transfers of small inorganic ions into DCM is expected at lower values than given above.

Data for the partition of the organic ion-pairs are shown in Table 1. Although only the decrease of the cation concentration was followed spectrophotometrically in the aqueous phase, the change of the $\log P'$ values with different counterions and the 1:50 value for the QA/organic counterion ratio strongly suggest that the quaternary amine cation enters the organic phase accompanied by the organic counterion. Since $P' < P$ (see eq 2),

$$\log P' < \log P = \log(c_o/c_w) = (G_w^\circ - G_o^\circ)/2.3RT \quad (4)$$

positive $\log P'$ values indicate larger standard free energy, G° , for the cation + anion system in water than in the water-saturated organic phase. In the majority of cases in Table 1, $\log P'$ is positive for octanol, and is above -1 with the DCM solvent. Even taking these negative values for $\log P$, which indicate preferable dissolution in water, there is still nonnegligible partition of the ion-pair in DCM for these systems.

The $\log P$ values are informative only regarding the c_o/c_w ratio, but tell nothing about the mechanism of the partitioning and the structure of the organic phase containing the cation + anion. Best et al.³⁶ found that ethylbenzene is located in the nonpolar region of the water-saturated *n*-octanol, but phenol associates with more polar regions of the solvent. At these sites the phenolic OH can form hydrogen bonds with both water and

(50) Dang, L. X. *J. Phys. Chem. B* **1999**, *103*, 8195.

the alcoholic OH of octanol. Bearing this modeling result in mind, one may expect the ionic sites of the ion-pair interacting with water and the octanol OH group, while the aliphatic chains could accommodate the nonpolar sites of both cation and anion. The question, however, whether the ion-pair dissolves in octanol in contact or separated form still remains unresolved. The water-saturated octanol may accommodate contact ion-pairs, but separated ions seem to disrupt the octanol structure to a lesser extent. In this case the separated ionic heads point into the water-filled bellies of octanol aggregates, and the nonpolar site(s) of the organic ions interact with each other and/or the octanol aliphatic chains. However, in the absence of any proof, we consider this model only as hypothetical.

More insight may be provided, upon the present modeling, for the DCM/water partition. On the basis of the PMF in Figure 7, the solvent-separated form with 9–10 Å separation of the (pyridine) N₅ atom of the homidium ion and the C₁ atom of the PTS anion is expected for these ions in water. The width of the water/DCM interface is about 8 Å.³⁷ It is unknown which ion enters the DCM phase first, but Dang's result⁵⁰ indicates smaller activation free energy for entering an anion rather than a cation. Assuming that the anion is the earlier entering unit, strongly bound water molecules are also expected to enter with the anion, forming hydrogen bonds to the SO₃⁻ site. The 9–10 Å separation of the ionic sites of the HOM-PTS (which is also favored in DCM) can be maintained when traversing the interface and both ions enter the DCM phase. Then the system either remains in solvent-separated form or after acquiring 2 kcal/mol activation free energy reaches stabilization in the contact ion-pair arrangement. The PMF predicts (if there is no significant further decrease of the curve) nearly equal concentration for the two forms in DCM in thermodynamic equilibrium at *T* = 298 °C.

Conclusions

Quaternary amines with organic counterions partition in *n*-octanol/water and dichloromethane/water systems. A good linear correlation (*r* = 0.945) of the log *P'* values was found when values determined in octanol/water and DCM/water systems were compared. The partitioned solutes must correspond to ion-pairs, because the quaternary substitution of the nitrogen atom ensures conservation of the positive charge on that unit. Correlation of the log *P* values obtained in different slightly polar solvents was pointed out previously for neutral molecules,³¹ as compared to the ion-pair partition in the present study.

Monte-Carlo simulation based PMFs in dichloromethane solvent indicate in general both locally stable contact and solvent-separated ion-pair arrangements. The solvent-separated form is at least as stable as the contact ion-pair. Consideration of two water molecules at the interaction sites of the ionic heads remarkably lowers the activation free energy toward the formation of the contact ion arrangement. The quaternary substitution of the nitrogen prevents hydrogen bonding to the cation at its most positive site. Secondary acceptor sites can still be important, but at larger separations the water molecules always formed strong hydrogen bonds only at the –COO⁻ and –SO₃⁻ anionic sites. The stability of the contact ion-pairs has been explained by the possible formation of water-bridged hydrogen bonds or water–benzene π -hydrogen bond.

The homidium-*p*-toluene sulfonate ion-pair is preferably separated in water. The contact form also corresponds to a local free energy minimum with, however, relative free energy of at least 5 kcal/mol at *T* = 298 °C. Contact and separated arrangements in DCM are equally stable. The activation free energy for the contact ion-pair is ~2 kcal/mol, the smallest for systems studied here.

Hydrogen bond analysis for the –NH₂ group of the aniline molecule concludes there is about 0.5 N···HO(water) bond in dilute aqueous solution. The result indicates, in accord with the experiment, that aniline is less basic than methylamine in aqueous solution. The –SO₃⁻ sites of the *p*-toluene sulfonate ion strongly bind 7–8 water molecules in hydrogen bonding with practically all of them.

According to a putative model suggested for the ion-pair partition between water and dichloromethane, the anion dragging some water molecules enters the organic phase first. The cation separated by about 8–10 Å follows the hydrated anion in the DCM phase. The ion-pair either remains in solvent separated form or reaches stabilization in the contact ion-pair form if the free energy difference does not exceed 2 kcal/mol, and the activation free energy of the contact ion-pair formation is no more than about 3 kcal/mol.

Acknowledgment. P. Nagy thanks Professor Jorgensen for the use of the BOSS 3.6 software. He also thanks the Ohio Supercomputer Center for the granted computer time used in performing ab initio calculations. The financial support of Hungarian National Scientific Foundation (OTKA I. 22623) for the experimental part of this work is also acknowledged by K. Takács-Novák.

JA000355I